

# Caracterización experimental y teórica de conexiones metálicas asimétricas susceptibles a falla de pernos

## Experimental and theoretical characterization of steel asymmetrical connections prone to bolt failure

J. Chanchi <sup>1\*</sup>, J. Castro \*, C. Gómez \*

\* Universidad Nacional de Colombia, Caldas, COLOMBIA

Fecha de Recepción: 29/07/2018  
Fecha de Aceptación: 20/12/2018  
PAG 193-204

### Abstract

*This article describes and proposes a model of the force versus elongation behaviour of asymmetrical connections prone to bolt failure when subjected to quasi-static axial load. 14 connections were assembled with one bolt varying the distance from the bolt to the edge of the clamped zone, and 14 connections were assembled with two bolts varying the distance between bolts. Results show that the axial force versus elongation behaviour of the connection is approximately trilinear, that while the connection stiffness is not sensitive to the bolt location in the clamped zone, the plastic elongation of the connection is. The model shows that the stiffness of the asymmetrical connection can be predicted from the stiffness of the connection components assessed by means of spring elements or beam elements, and that the load capacity of the connection can be predicted using the dry friction theory of Coulomb and the shear bolt capacity.*

*Keywords: Steel connection, Asymmetrical connection, Distance between bolts, Distance from bolt to edge, Asymmetrical connection stiffness*

### Resumen

El Este artículo describe y propone un modelo del comportamiento fuerza contra elongación de conexiones metálicas asimétricas susceptible a falla de pernos cuando sometidas a carga axial cuasi-estática. 14 conexiones se ensamblaron con un perno variando la distancia desde el perno al borde de la zona de unión de las platinas y 14 conexiones se ensamblaron con dos pernos variando la distancia entre pernos. Los resultados experimentales muestran que el comportamiento fuerza axial contra elongación de la conexión es aproximadamente trilineal y que mientras la rigidez de la conexión no es sensible a la localización de los pernos en la zona de unión de las platinas; la elongación plástica de la conexión si lo es. El modelo muestra que la rigidez de la conexión asimétrica se puede predecir evaluando la rigidez de los componentes de la conexión usando elementos de resorte y viga y que la capacidad de carga de la conexión se puede predecir con base en la teoría de la fricción seca de Coulomb y la capacidad a corte de los pernos.

**Palabras clave:** Conexión metálica, Conexión asimétrica, Distancia entre pernos, Distancia desde el perno al borde, Rigidez de conexión asimétrica

## 1. Introduction

Bolted steel connections that allow for the transfer of axial loads through shear and compressive stresses are called shear joints. According to the configuration of the members that these connections hold together, these connections are classified into either symmetrical or asymmetrical. While in symmetrical connections, a central member transfers the load to two external members, in the asymmetrical connections the load is transferred between two members only (Bresler et al., 1968). These two kinds of connections can be used in different structural systems in a conventional way, to simply connect structural members, or in a sophisticated manner, as a mechanism for seismic energy dissipation (Grigorian and Popov, 1994) (Clifton, 2005). In conventionally-used connections, the design is ruled solely by the load capacity associated to failure limit states, and it does not attach much importance to the connection stiffness. In fact, when

structural systems are analyzed and designed, the connection stiffness is not considered, since their analysis is complex and indeterminate. In this perspective, they are considered very rigid elements when compared with the structural system (Trahair and Bradford, 1988) (McGuire, 1968). When the connection stiffness quantification is regularly required, sophisticated numerical methods are used, such as the finite element analysis validated from experimental data such as those reported by (Clifton, 2005) in relation to asymmetrical connections. This methodology should be followed, not only because the load transfer mechanism of connections is complex, but also because the mechanism is sensitive to the presence of holes and the possible yield strength of the connection components (Gorenc and Tinyou, 1984). Given the lack of a simple methodology, which does not require sophisticated numerical models for quantifying the stiffness of asymmetrical connections, this paper proposes a simple methodology for assessing the stiffness of this kind of connection, validated by experimental data and using a simple elasticity theory, as suggested by (Schenker et al., 1954) and (Grigorian and Popov, 1994) in the stiffness assessment of symmetrical connections. The present paper seeks to answer the following questions:

<sup>1</sup> Corresponding author:

Universidad Nacional de Colombia, Caldas, COLOMBIA  
E-mail: jcchanchigo@unal.edu.co



- i. What is the axial force vs. elongation behavior of the asymmetrical connection liable to suffer bolt failure?
- ii. What is the effect of varying the bolt location in the clamping zone on the trend of the axial force vs. elongation curve and on the deformability of the asymmetrical connection liable to bolt failure?
- iii. Which is a theoretical model for estimating the load capacity of the asymmetrical connection liable to bolt failure?
- iv. Which is a theoretical model for estimating the stiffness of the asymmetrical connection liable to bolt failure?

- v. Which is a theoretical model representing the axial force vs. elongation behavior of the asymmetrical connection liable to bolt failure?

## 2. Materials

The asymmetrical joint was built with one fixed and one moving plate connected by bolts in an area called clamping zone. A first type of connection, called Assembly 1, was built by connecting the plates with a bolt and varying the distance between the edge of the bolt hole and the edge of the clamping zone ( $B$ ) (Figure 1a).

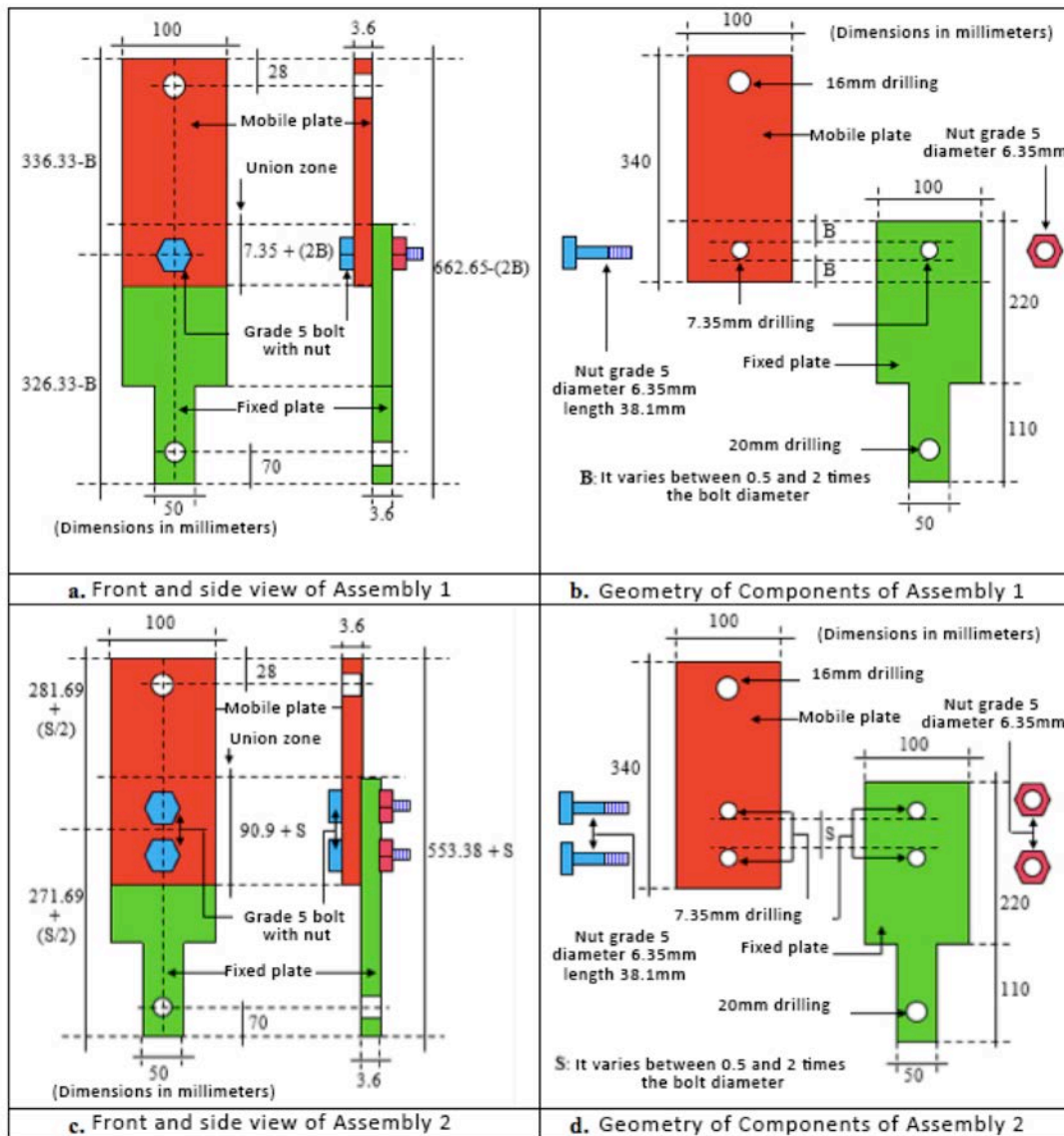


Figure 1. Geometry of the connection components and Assemblies 1 and 2

A second type of connection, called Assembly 2, was built by connecting the plates with two bolts, varying the distance between bolt hole edges ( $S$ ) and keeping constant the distance between the edge of bolt holes and the edge of the clamping zone (Figure 1c). In both assemblies, the fixed and moving plates were manufactured with steel A36 (yield strength of 250MPa, ultimate strength of 410 MPa). The dimensions of the fixed and moving plates in both assemblies are shown in (Figure 1). The bolts in the clamping zone were made of heat-treated medium carbon steel, type SAE Grade 5 (test strength of 595 MPa, ultimate strength of 840 MPa) with diameter of 6.35 mm and length of 38.1 mm. The bolts were assembled using a nut only and they were tensioned to the test load using the Turn-of-Nut method (Figure 1). In both

assemblies, the connections were designed for the bolt to fail at shear stress before the plates underwent tensile strength failure, and the hole edges should be liable to visually perceptible compressive deformations.

### 3. Test methods

#### 3.1 Description of the Assembly

Each connection was tested in a vertically-arranged assembly on a servo driven hydraulic press, where the connection was provided with one fixed and one moving support (Figure 2a) (Figure 2b).



Figure 2. Connection test assembly



The fixed support of the connection was set by restraining the vertical displacement of the fixed plate by means of a fixed rod passing through the fixed plate, and supported by the lower face of the drilled plate (Figure 2c). The moving support of the connection was set by connecting the actuator to the moving plate through a metal housing with a floating rod (Figure 2b) (Figure 2d). This assembly was set out with a load cell connected in series to the actuator and an extensometer located close to the connection (Figure 2a) (Figure 2b) (Figure 2c) (Figure 2d).

### 3.2 Number of Tests and Methodology Used

In total, 28 tests were carried out, distributed in 14 tests in Assembly 1 and 14 tests in Assembly 2 (Table 2). The

14 tests of Assembly 1 were divided into 7 groups, where the distance between the edge of the bolt hole and the edge of the clamping zone ( $B$ ) was changed based on the number of times of a 6.35 mm bolt diameter ( $\emptyset$ ) (Table 1). The 14 tests of Assembly 2 were divided into 7 groups, where the distance between edges of bolt holes in the clamping zone ( $S$ ) was changed based on the number of times of a 6.35mm bolt diameter ( $\emptyset$ ) (Table 1) and the distance from the hole edge to the edge of the clamping zone was kept constant and equal to six times the bolt diameter. In each test, the connection was axially loaded in a quasi-static way at a speed of 10 mm/s from a null load to the load inducing the bolt to failure. A new set of plates and bolts was used for each assembly and in every test.

**Table 1.** Number of tests per connection assembly

ASSEMBLY 1			ASSEMBLY 2		
$B$ expressed in mm and in number of times a 6.35mm bolt diameter ( $\emptyset$ )		Number of tests	$S$ expressed in mm and in number of times a 6.35mm bolt diameter ( $\emptyset$ )		Number of tests
mm	#	#	mm	#	#
6.35	1.0 $\emptyset$	2	3.18	0.5 $\emptyset$	2
7.94	1.25 $\emptyset$	2	4.76	0.75 $\emptyset$	2
9.53	1.5 $\emptyset$	2	6.35	1.0 $\emptyset$	2
11.11	1.75 $\emptyset$	2	7.94	1.25 $\emptyset$	2
12.70	2.0 $\emptyset$	2	9.53	1.5 $\emptyset$	2
15.88	2.5 $\emptyset$	2	11.11	1.75 $\emptyset$	2
19.05	3.0 $\emptyset$	2	12.70	2.0 $\emptyset$	2
Total tests		14	Total tests		14

## 4. Results and analysis

### 4.1 Axial Force vs. Elongation Behavior of the Asymmetrical Connection

(Figure 3) shows that the global trend of the axial force vs. elongation curve of the connection is similar in Assemblies 1 and 2. This similarity indicates that the trend of the axial force vs. elongation curve is not sensitive to the

number nor the location of bolts in the clamping zone. Three, almost linear, trend zones define the axial force vs. elongation curve (Figure 3). The first or pre-sliding zone, since no apparent plate movement nor a contact between the plate and the bolt rod were observed. In this zone, the connection shows its maximum stiffness and the connection behavior is ruled by the elastic behavior of the plates and fasteners (Figure 3).

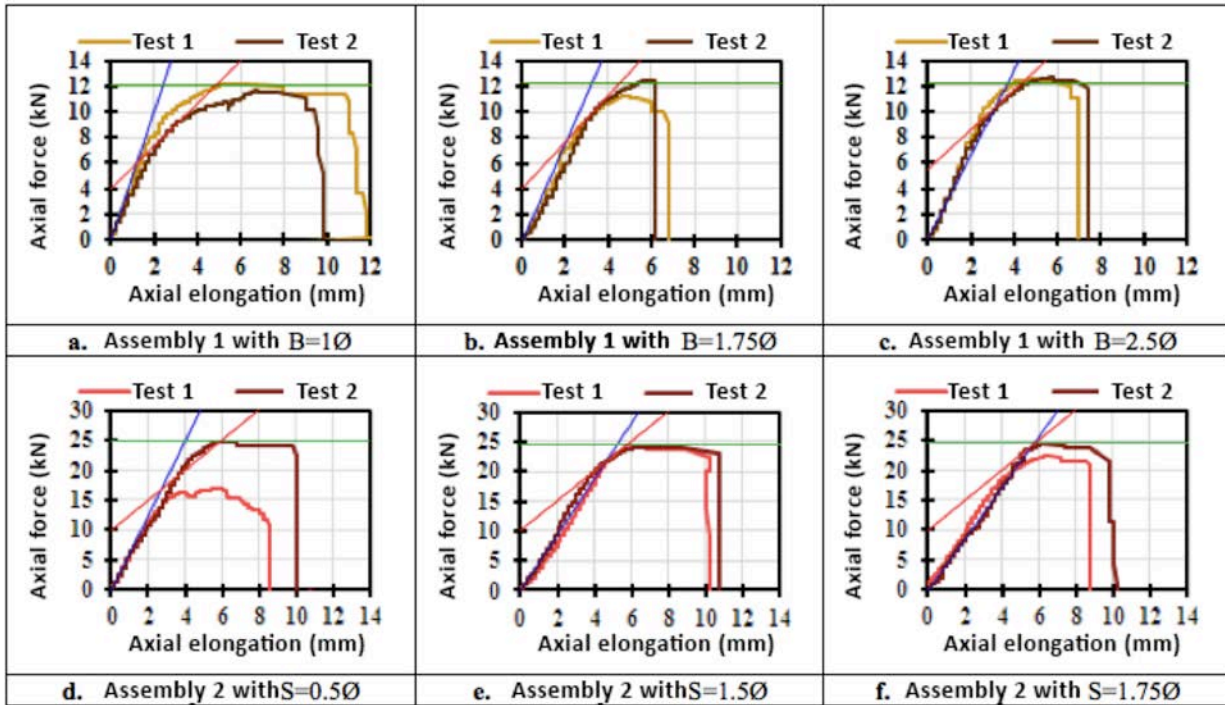


Figure 3. Axial force vs. elongation curve of Assemblies 1 and 2

The second or post-sliding zone, since the moving plate slides until touching the bolt rod, thereby producing the displacement of the bolts along the hole. While plates and fasteners behave elastically, bolts behave elastically at the beginning of the zone and reach the yield point at the end of the zone. The connection evidences a stiffness reduction not only due to the fact that bolt stiffness is small compared with the stiffness of plates and fasteners, but also because bolts begin to yield (Figure 3). In the third or plastic zone, the connection stiffness is null because the bolts totally yield to shear failure and the hole zones in contact with the bolts reach the yield point due to the concentration of compressive stresses transferred by the bolts. Once the bolts undergo shear failure, the connection is completely unloaded (Figure 3).

#### 4.2 Deformability in Boreholes

After the test, the fixed plates were removed in both Assemblies 1 and 2. The (Figure 4) shows the clamping zone of the removed fixed plates and the respective axial force vs. elongation curves for both assemblies. It is possible to observe that the maximum deformability in the boreholes occurred in the connection with minimum spacing between the edge of the bolt hole and the edge of the clamping zone (Figure 4a) and in the connection with the minimum spacing between edges of bolt holes in the clamping zone (Figure 4d). Both assemblies also reveal that these increased distances reduced the deformability in the boreholes (Figure 4b) (Figure 4e) and that deformabilities are small for distances over 1.75 times the bolt diameter (Figure 4c) (Figure 4f).

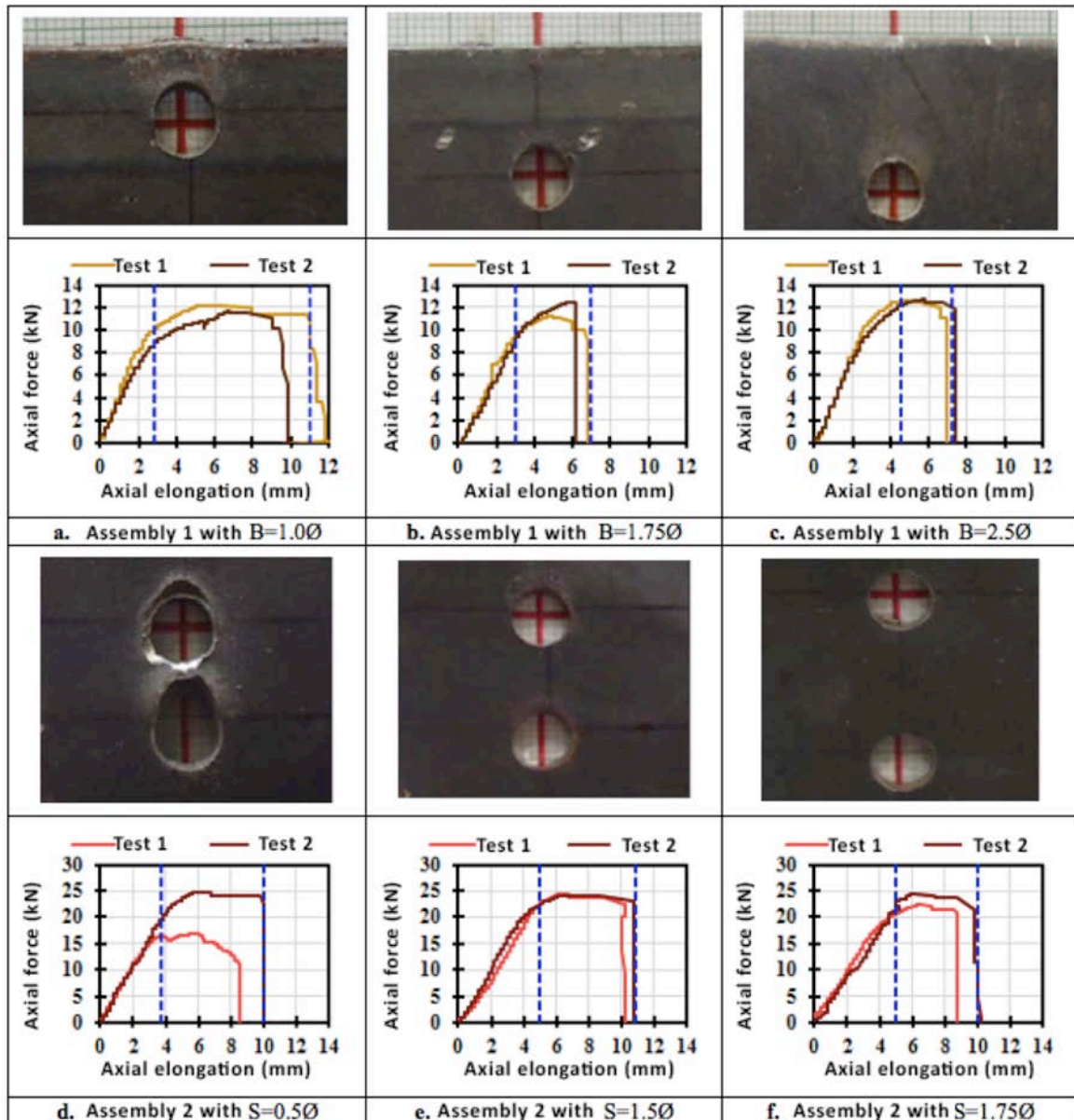


Figure 4. Axial force vs. elongation curve and deformability of the boreholes in Assemblies 1 and 2

The (Figure 4) shows that the increase of these distances reduces the amplitude of the plastic zone of the axial force vs. elongation curve. This reduction of the plastic zone occurs because, when increasing these distances, the compressive stresses of the bolts on the plates are distributed in broader areas, thus reducing the deformability of the areas close to the holes.

## 5. Development of the Tehorical Model

### 5.1 Load Capacity of the Asymmetrical Connection

The load capacity of the connection was defined based on the force that initiates the sliding of the moving

plate, called sliding triggering force, and the force producing the bolt failure.

#### 5.1.1 Sliding Triggering Force

The sliding triggering force of the moving plate was modeled considering that sliding triggers when the friction in the interface between the fixed and the moving plate is exceeded. The friction force was assessed using Coulomb's dry friction theory (Equation 1), where the friction force ( $F$ ) is proportional to a friction coefficient in the interface of the surfaces where the sliding is produced ( $\mu$ ) and to the regular force between surfaces ( $N$ ) (Popov, 2010). In asymmetrical connections, this theory was applied considering the friction coefficient between the fixed and the moving plate, and considering the regular force between the fixed and the moving surface as the product of the number of bolts ( $m$ ), the

ENGLISH VERSION.....

number of friction interfaces ( $n$ ) and the tensile strength induced on each bolt when assembling the connection ( $T$ ) (Equation 2).

$$F = \mu \times N \quad (1)$$

$$F = \mu \times [m \times n \times T] \quad (2)$$

### 5.1.2 The Force Inducing Bolt Failure

The force inducing bolt failure ( $F_u$ ) was modeled considering that bolts fail when the fixed and the moving plate make contact with the bolts, thereby producing shear forces exceeding the shear strength in the bolts' threaded zone. The bolts' ultimate shear force ( $\tau$ ) was considered proportional to the bolts' ultimate tensile stress ( $\sigma$ ) through a dimensionless factor ( $\phi$ ) of 0.6, following the theory of Von

Mises (Beer et al., 2010) (Equation 3). The ultimate shear strength in the bolts' threaded zone ( $R$ ) was calculated as the product between the ultimate shear force and the effective area in the bolts' threaded zone expressed as a reduction of the gross area ( $A_{bolt}$ ) through a dimensionless factor ( $\beta$ ) of 0.7 (Equation 4).

$$\tau = \phi \times \sigma \quad (3)$$

$$F_u = \tau \times (\beta \times A_{bolt}) \quad (4)$$

### 5.2 Stiffness of the Asymmetrical Connection

The connection was divided into four components: the fixed and moving plate set, the fixed fastener, the floating fastener and the bolts in the clamping zone (Figure 5).

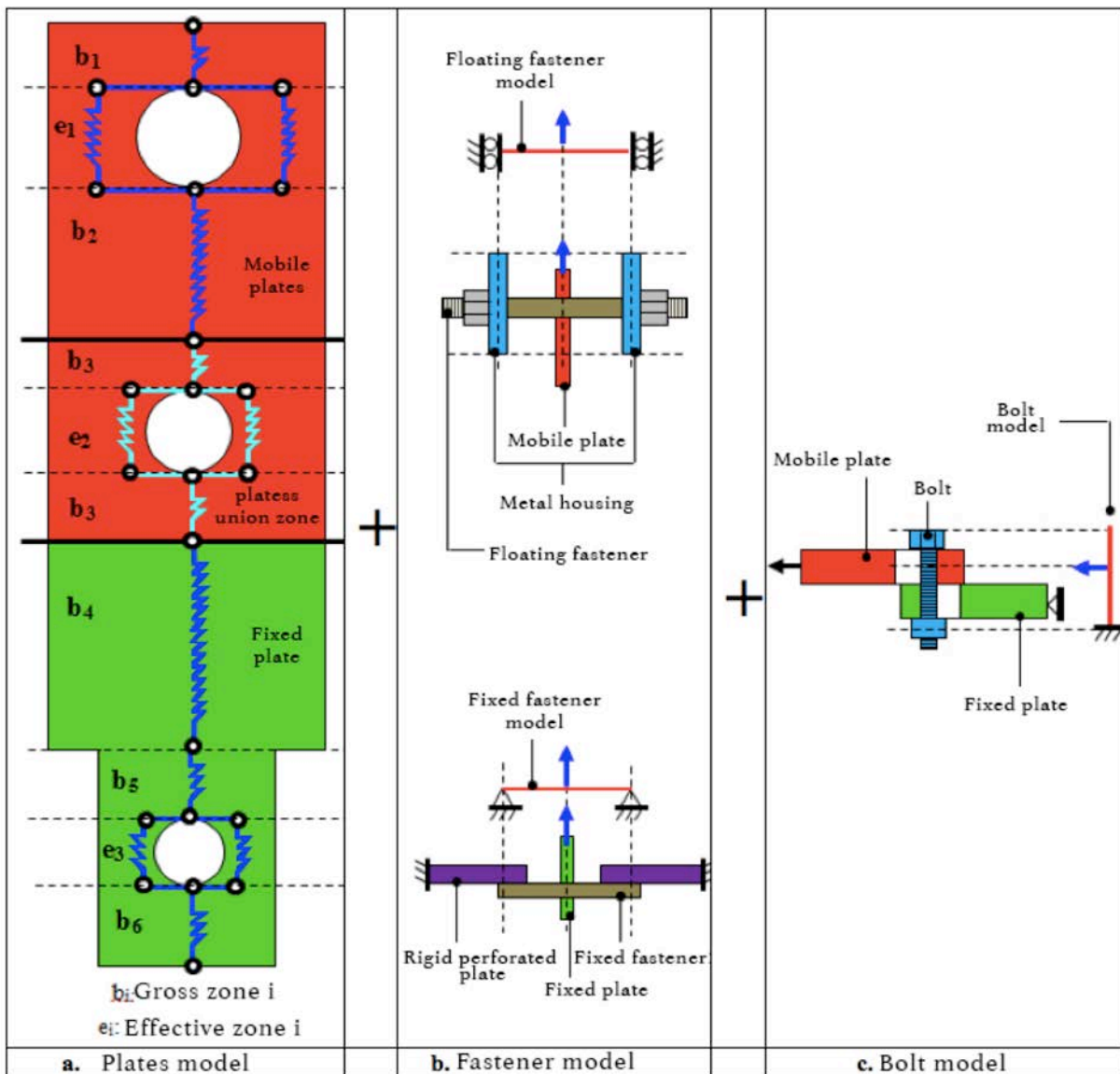


Figure 5. Connection stiffness



The connection stiffness ( $K$ ) was assessed by connecting in series the stiffness of the fixed and moving plate set ( $K_{plates}$ ), the stiffness of the fixed fastener ( $K_{fixed-fastener}$ ), the stiffness of the floating fastener ( $K_{floating-fastener}$ ) and the stiffness of the bolts in the clamping zone ( $K_{bolts}$ ) (Equation 5).

$$K = \frac{1}{\frac{1}{K_{plates}} + \frac{1}{K_{fixed-fastener}} + \frac{1}{K_{floating-fastener}} + \frac{1}{K_{bolts}}} \quad (5)$$

### 5.2.1 Plate Stiffness

The stiffness of the fixed and moving plate set was assessed by discretizing the set in a succession of plate fractions, called effective and gross, which were assigned to plate zones with and without drilling, respectively. Gross plate fractions were represented by one spring and effective plate fractions were represented by two springs, one on each side of the hole (Figure 5a). The stiffness of each spring ( $K_i$ ) was assessed based on the plate fraction area ( $A_i$ ), the modulus of elasticity ( $E_i$ ) and the plate fraction length ( $L_i$ ) (Equation 6). The stiffness of the fixed and moving plate set ( $K_{plate}$ ) was assessed by connecting in series the stiffness of the springs that represented the effective plate fractions ( $k_{e_i}$ ) and the stiffness of the gross plate fractions ( $k_{b_i}$ ) (Equation 7).

$$K_i = \frac{A_i \times E_i}{L_i} \quad (6)$$

$$K_{plates} = \frac{1}{\sum \left[ \frac{1}{K_{e_i}} \right] + \sum \left[ \frac{1}{K_{b_i}} \right]} \quad (7)$$

### 5.2.2 Stiffness of Fixed and Floating Fasteners

The stiffness of fixed and floating fasteners were calculated considering that they behave as a simply supported beam subjected to a load in the center of the span, which corresponds to the load transferred by the fixed plate to the moving plate in the center of the corresponding fastener (Figure 5b). The stiffness of each fastener ( $K_{fastener}$ ) was assessed using the modulus of elasticity of the fastener ( $E_{fastener}$ ), the fastener inertia ( $I_{fastener}$ ) and the distance between fastener supports ( $L_{fastener}$ ) (Equation 8).

$$K_{fastener} = \frac{48 \times E_{fastener} \times I_{fastener}}{L_{fastener}^3} \quad (8)$$

### 5.2.3 Bolt Stiffness in the Clamping Zone

The bolt stiffness was calculated considering that the bolt behaves as a cantilever beam embedded in the middle of the nut's thickness, with free end in the upper part of the bolt

head and subjected to a precise load in the middle of the moving plate thickness corresponding to the load transferred by the moving plate to the bolt when they make contact (Figure 5c). The bolt stiffness was assessed using the modulus of elasticity of the bolt ( $E_{bolt}$ ), the bolt inertia ( $I_{bolt}$ ), the distance from the middle of the nut thickness to the upper part of the bolt head ( $L_{bolt}$ ) and the distance from the center of the nut thickness to the center of the moving plate thickness ( $a_{bolt}$ ) (Equation 9).

$$K_{bolt} = \frac{6 \times E_{bolt} \times I_{bolt}}{a_{bolt}^2 \times [(3 \times L_{bolt}) - a_{bolt}]} \quad (9)$$

### 5.3 Theoretical Model of the Axial Force vs. Elongation Curve of the Connection

The axial force vs. elongation curve of the connection was represented by a trilinear model (Figure 6a). The first or pre-sliding zone is limited by the sliding triggering force (Figure 6a), and the stiffness ( $K_{pre-sliding}$ ) corresponds to the interaction in series of the stiffness of the fixed and moving plate set and the fixed and floating fasteners (Equation 10). This stiffness represents the case where the fixed and moving plate set and the fasteners are elastically deformed without the interaction of the bolts' rod (Figure 6b). The second or post-sliding zone, is limited on the lower side by the sliding triggering force and, in the upper side, by the force inducing bolt failure (Figure 6a), and the stiffness ( $K_{post-sliding}$ ) corresponds to the interaction in series of the stiffness of the fixed and moving plate set, the fixed and floating fasteners, and the bolts (Equation 11). This stiffness represents the case where the moving plate slides until making contact with the bolt rods, making the bolts to slide along the hole. In this case, all connection components behave elastically until the bolts begin to yield (Figure 6c).

$$K_{pre-sliding} = \frac{1}{\frac{1}{K_{plates}} + \frac{1}{K_{fixed-fastener}} + \frac{1}{K_{floating-fastener}}} \quad (10)$$

$$K_{post-sliding} = \frac{1}{\frac{1}{K_{plates}} + \frac{1}{K_{fixed-fastener}} + \frac{1}{K_{floating-fastener}} + \frac{1}{K_{bolts}}} \quad (11)$$

The third or plastic zone is limited by the force inducing bolt failure and presents a null stiffness since the bolts yield to failure (Figure 6a). The extension of this zone is ruled by the deformability of the bolts subjected to bending stresses and the deformability of the borehole areas in contact with the bolts subjected to compressive stresses transferred by the bolts (Figure 6d).

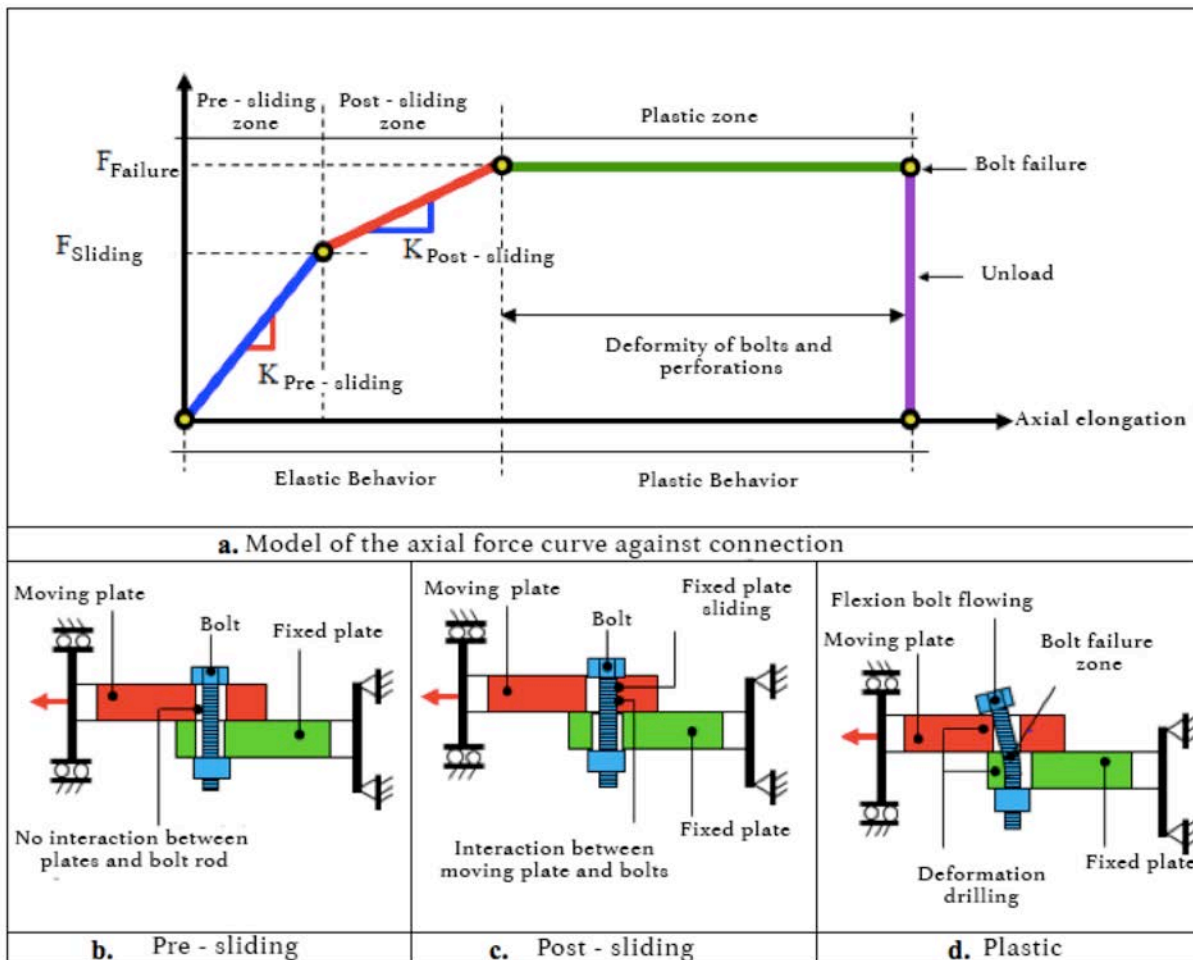


Figure 6. Model of the connection behavior to axial force

## 6. Correlation

In both Assemblies 1 and 2, the axial force vs. elongation curve model described in Section 5 was implemented. The sliding triggering force was calculated considering a friction coefficient ( $\mu$ ) of 0.30 corresponding to the dynamic friction reported by (Chanchí et al., 2012) and considering a friction interface, which corresponds to the

interface between the fixed and the moving plate. The force inducing the bolt failure was calculated considering an ultimate tensile stress of the bolts ( $\sigma$ ) of 900 MPa, corresponding to the value reported by the manufacturer (Gutiérrez, 2000). The (Table 2) shows a summary of the implementation of the axial force vs. elongation curve model for Assembly 2, with a distance between edges of bolt holes of 1.25 times the bolt diameter ( $S=1.25$ ).

**Table 2.** Implementation of the Assembly 2 model with  $S=1.25$

		Área	Length	Modulus of elasticity	Stiffness
		mm <sup>2</sup>	mm	MPa	kN/mm
Gross areas	b1	360.0	20.0	200000.0	3600.0
	b2	360.0	205.2	200000.0	351.0
	b3	720.0	38.1	200000.0	3779.5
	b4	720.0	7.9	200000.0	18471.7
	b5	187.2	30.0	200000.0	594.2
	b6	187.2	60.0	200000.0	1248.0
	b7	187.2	60.0	200000.0	624.0
Effective areas	e1	302.4	16.0	200000.0	3780.0
	e2	1176.7	7.4	200000.0	32017.8
	e3	115.2	20.0	200000.0	1152.0
Fixed fastener	Modulus of elasticity		E	MPa	200000.0
	Inertia		I	mm <sup>4</sup>	1277.0
	Length		Lp	mm	65.0
Floating fastener	Modulus of elasticity		E	MPa	200000.0
	Inertia		I	mm <sup>4</sup>	523.0
	Longitud		Lp	mm	100.0
Bolt	Diameter		d	mm	6.4
	Inertia		I	mm <sup>4</sup>	19.2
	Modulus of elasticity		E	MPa	200000.0
	Distance from half the thickness of the nut to the top of the head of the bolt		L	mm	14.0
	Distance from the center of the nut thickness to the center of the mobile plate thickness		a	mm	8.2
Components stiffness	Plates		$K_{plates}$	kN/mm	111.0
	Fixed fastener		$K_{fastener}$	kN/mm	44.7
	Floating fastener		$K_{fastener}$	kN/mm	5.0
	Bolt		$K_b$	kN/mm	10.2
Strength	Force that activate the slide		F	kN	7.9
	Bolt failing force		R	kN	24.0
Conection stiffness	Pre-sliding		$K_{pre-sliding}$	kN/mm	5.4
	Post-sliding		$K_{post-sliding}$	kN/mm	2.6
	Yielding		$K_{yielding}$	kN/mm	0.0

According to the methodology presented in (Table 2), the variables defining the axial force vs. elongation curve were determined for both Assemblies 1 and 2. The (Figure 7)

shows the axial force vs. elongation curve for Assemblies 1 and 2 overlapped with experimental data.

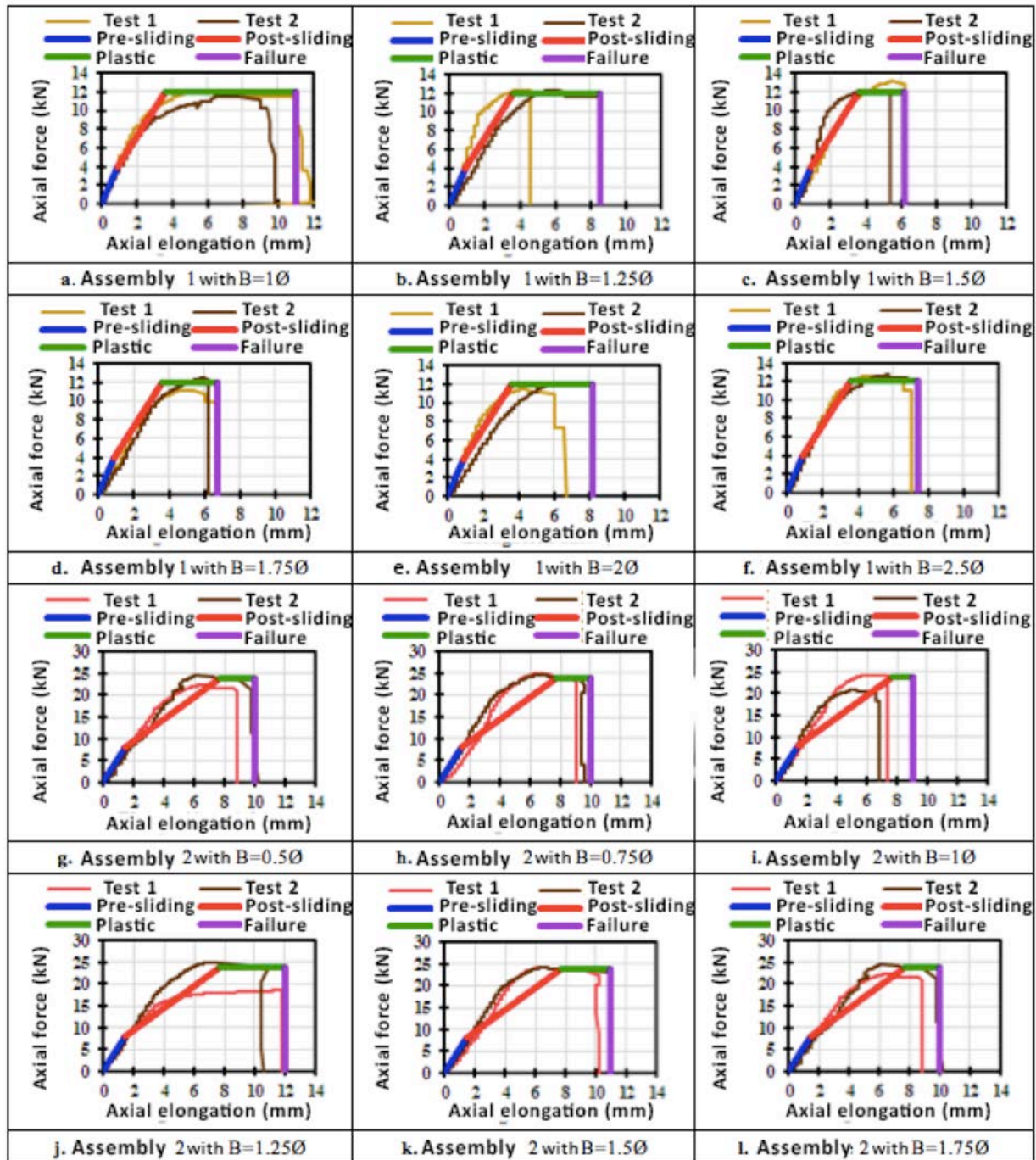


Figure 7. Correlation between the theoretical model and the experimental results for asymmetrical connection in Assemblies 1 and 2

The (Figure 7) allows observing that the model predicts the post-sliding and plastic zones of the experimental data with a good approximation. However, the model predicts the stiffness of the post-sliding zone with an acceptable approximation. This discrepancy is due to the fact

that the stiffness model of the post-sliding zone was based on the assumption that bolts behave elastically throughout the entire post-sliding zone. This assumption is only valid for the beginning of the zone, when the plate makes contact with the bolts, and not for the end when the bolts reach the yield



point. Additionally, the bolts do not simultaneously reach the yield point nor their yield point occurs exactly at the end of the post-sliding zone, because the Turn-of-Nut method used during the assembly does not accurately guarantee the bolts' tensioning level.

## 7. Conclusions

This paper experimentally describes and proposes a theoretical model for axial force vs. elongation behavior of asymmetrical connections liable to bolt failure. The following was demonstrated:

- i. The axial force vs. elongation behavior of the connection is characterized by three zones with linear trend. In the first or pre-sliding zone, the connection shows its maximum stiffness with apparently no movement of the plates. In the second or post-sliding zone, the connection shows a stiffness reduction due to the moving plate sliding until making contact with the bolt rod. And in the third or plastic zone, the connection stiffness is null due to the yield strength of the bolts and the areas close to the bolt holes.
- ii. The global trend of the axial force vs. elongation curve of the connection is not sensitive to the bolt location in the clamping zone. However, the amplitude of the plastic zone is. The increase of the distance between the edge of the bolt hole and the edge of the clamping zone and the increase of the distance between edges of bolt holes decreases the axial deformability of the connection, the deformability of bolt holes and the amplitude of the plastic zone.
- iii. The load capacity of the connection can be described by the sliding triggering force and the force inducing bolts to fail. The sliding triggering force can be modeled with Coulomb's dry friction theory, considering that this force is proportional to the tensioning force of the bolts and to the friction coefficient in the interface between the fixed plate and the moving plate. The force inducing bolt failure can be modeled considering that this force is proportional to the tensile strength of bolts reduced by a factor of 0.6.
- iv. The connection stiffness can be analyzed by connecting in series the stiffness of each component assessed by the stiffness of beam elements or spring elements. The stiffness of beam elements can be used in components subjected to bending, as in the case of bolts and fasteners. The stiffness of spring elements can be used in components subjected to axial force, as in the case of plates.
- v. The axial force vs. elongation behavior of the connection can be represented by a trilinear model formed by the pre-sliding zone, the post-sliding zone and the plastic zone. These zones are delimited by the sliding triggering force and the force inducing bolt failure. The assessment of the stiffness in the pre-sliding zone considers the stiffness of plates and fasteners, and the assessment of the stiffness in the post-sliding zones considers the stiffness of plates, fasteners and bolts. The stiffness of the plastic zones is considered null.

## 8. Referencess

- Beer, F. P., Johnston, E. R., DeWolf, J. T., Mazurek, D. F., (2010).** Mecánica de Materiales, p. 791, México, D. F.- México: McGraw-Hill. \*p. 452.
- Bresler, B., Lin, T. Y., Scalzi, J. B. (1968).** Design of Steel Structures, p. 830, New York - United States of America: John Wiley & Sons, Inc. \*p. 111, 113, 118, 119.
- Chanchí, J., MacRae, G. A., Chase, J. G., Rodgers, G. W., Clifton, G. C. (2012, 13 de abril).** Behaviour of Asymmetrical Friction Connections Using Different Shim Materials. New Zealand Society for Earthquake Engineering – Annual Technical Conference. Christchurch – New Zealand.
- Clifton, G.C. (2005).** Semi-Rigid Joints for Moments Resisting Steel Framed Seismic Resisting Systems. Published PhD Thesis. Auckland – New Zealand: University of Auckland. Department of Civil and Environmental Engineering.
- Gorenc, B. E., Tinyou, R. (1984).** Steel Designers Handbook, p. 336, New South Wales - Australia: New South Wales University Press Ltda. \*p. 41, 42, 46.
- Grigorian, C. E., Popov, E. P., (1994).** Energy Dissipation with Slotted Bolted Connections, p. 234, Berkeley – United States of America: College of engineering, University of Berkeley. \*p. 9,10.
- Gutiérrez, H. (2000).** Manual de tornillos, pernos y tuercas, p. 63, Bogotá – Colombia. \*p. 10.
- McGuire, W. (1968).** Steel Structures, p.1112, United States of America: Prentice Hall, Inc. \*p.787, 788.
- Popov, V. L. (2010).** Contact Mechanics and Friction. Physical Principles and Applications, p. 362, New York - United States of America: Springer. \*p. 134.
- Schenker, L., Salmon, C. G., Johnston, B. G. (1954).** Structural Steel Connections, p. 256, Michigan – United States of America: University of Michigan. \*p. II-26, II- 27, II-28.
- Trahair, N. S., Bradford, M. A. (1988).** The Behaviour and Design of Steel Structures, p. 391, Sidney – Australia: Methuen of Australia. \*p. 359, 362, 363, 364.